Special Issue Article

Institution of MECHANICAL ENGINEERS

Journal of ENGINEERING IN MEDICINE

Proc IMechE Part H:
J Engineering in Medicine
1–10
© Authors 2015
Reprints and permissions:
sagepub.co.uk/journalsPermissions.nav
DOI: 10.1177/0954411915602915
pih.sagepub.com
SAGE

Effect of calcium/sodium ion exchange on the osmotic properties and structure of polyelectrolyte gels

Ferenc Horkay[1], Peter J Basser[1], Anne-Marie Hecht[2] and Erik Geissler[2]

Abstract

We discuss the main findings of a long-term research program exploring the consequences of sodium/calcium ion exchange on the macroscopic osmotic and elastic properties, and the microscopic structure of representative synthetic polyelectrolyte (sodium polyacrylate, (polyacrylic acid)) and biopolymer gels (DNA). A common feature of these gels is that above a threshold calcium ion concentration, they exhibit a reversible volume phase transition. At the macroscopic level, the concentration dependence of the osmotic pressure shows that calcium ions influence primarily the third-order interaction term in the Flory–Huggins model of polymer solutions. Mechanical tests reveal that the elastic modulus is practically unaffected by the presence of calcium ions, indicating that ion bridging does not create permanent cross-links. At the microscopic level, small-angle neutron scattering shows that polyacrylic acid and DNA gels exhibit qualitatively similar structural features in spite of important differences (e.g. chain flexibility and chemical composition) between the two polymers. The main effect of calcium ions is that the neutron scattering intensity increases due to the decrease in the osmotic modulus. At the level of the counterion cloud around dissolved macroions, anomalous small-angle X-ray scattering measurements made on DNA indicate that divalent ions form a cylindrical sheath enveloping the chain, but they are not localized. Small-angle neutron scattering and small-angle X-ray scattering provide complementary information on the structure and interactions in polymer solutions and gels.

Keywords

Polymer gel, biomimetics, ions, osmotic pressure, small-angle scattering, DNA, polyacrylic acid

Date received: 9 March 2015; accepted: 20 July 2015

Introduction

Negatively charged polyelectrolyte gels exhibit a reversible volume transition from the swollen to the collapsed state when monovalent ions are replaced by divalent counterions.[1–5] In many systems, this transition is abrupt and can be initiated by a small change in the ionic composition of the equilibrium solution. It is also known that such reversible volume changes are common in a variety of biological processes, such as nerve excitation. For example, Tasaki et al.[6–12] studied nerve excitation from a polymer physics perspective. He argued that electrophysiological processes known as "nerve excitation and conduction" are, basically, manifestations of abrupt structural changes in the cortical gel layer of nerve fibers and demonstrated that several aspects of this excitation phenomena could be reproduced using synthetic polyanionic hydrogels.

In neutral polymer gels, phase transition can be induced only by decreasing the thermodynamic quality of the solvent (e.g. by adding a nonsolvent or changing the temperature). However, in polyelectrolytes, addition of salt can also lead to collapse of the polymer chains.

Phase transition of polyelectrolyte solutions and gels has been the subject of many theoretical and experimental studies.[13–17] The majority of previous works have focused either on the salt-free case or on the effect of monovalent salts. These experiments can be interpreted in terms of the Poisson–Boltzmann model. Relatively,

[1]Section on Tissue Biophysics and Biomimetics, Eunice Kennedy Shriver National Institute of Child Health and Human Development, National Institutes of Health, Bethesda, MD, USA
[2]Laboratoire Interdisciplinaire de Physique (LIPhy), Université Grenoble Alpes, CNRS, Grenoble, France

Corresponding author:
Ferenc Horkay, Section on Tissue Biophysics and Biomimetics, Eunice Kennedy Shriver National Institute of Child Health and Human Development, National Institutes of Health, Bldg. 13, Room 3W16, 13 South Drive, Bethesda, MD 20892, USA.
Email: horkayf@helix.nih.gov

little attention has been paid to the biologically more relevant situation when both mono- and divalent counterions are present.

Previous results show that divalent counterions strongly affect the macroscopic properties (e.g. swelling degree) of polyelectrolyte gels, and above a threshold concentration, these ions lead to a volume transition.[3–5,18,19] However, it is much less understood how divalent/monovalent ion exchange affects the thermodynamic interaction between the polymer and the solvent. Since anionic polymer chains can be linked together by multivalent cations, the observed volume transition in polyelectrolyte systems is frequently attributed to ion bridging between charged groups that are located on neighboring chains. Investigations by small-angle scattering techniques and mechanical measurements can cast light on these questions.

The aim of this article is to explore the effect of calcium ions on the thermodynamic and mechanical properties of polyelectrolyte gels at different length scales and to identify changes in the supramolecular structure of the polymer due to divalent/monovalent ion exchange. We investigate DNA and polyacrylic acid (PAA) gels swollen in NaCl solution in the presence of different amounts of $CaCl_2$, using small-angle neutron scattering (SANS) together with mechanical and thermodynamic (osmotic) observations. An attempt is made to separate ion bridging from ion-induced changes in the thermodynamic interactions. We also report anomalous small-angle X-ray scattering (ASAXS) measurements that make it possible to determine the counterion distribution in the ion cloud surrounding DNA molecules. The counterion distribution around DNA is correlated with the macroscopic thermodynamic parameters determined from osmotic pressure measurements.

Experimental

Materials

DNA solutions were made from a sodium salt of DNA (Sigma, salmon testes, $M_w = 1.3 \times 10^6$) in NaCl solution. The percentage of G–C content of this DNA is 41.2%. Different amounts of calcium chloride were added to the DNA solutions. Solutions containing 3% w/w DNA were cross-linked with ethylene glycol dimethyl ether at pH 8.5 in the presence of tetramethylethylenediamine (TEMED).[2]

Sodium polyacrylate gels were synthesized with 0.3% w/w by weight of the cross-linker N,N′-methylenebis(acrylamide) in aqueous solution as described previously.[5] The acrylic acid units were first neutralized in NaOH and equilibrated with aqueous solutions of NaCl. In all samples, the pH was 7, where both DNA and PAA are fully dissociated.

Swelling pressure and mechanical measurements

Swelling pressure and mechanical measurements were made by the osmotic stress technique. Gels were equilibrated with poly(vinyl pyrrolidone) (PVP) solutions (molecular weight: 29 kDa) of known osmotic pressure.[20,21] A semipermeable membrane was used to separate the gel from the polymer solution. After attaining equilibrium (approximately 4–5 days), the concentrations of the polymers were measured in both phases.

The shear modulus of the gels was determined using a TA.XT2I HR Texture Analyzer (Stable Micro Systems, UK). Measurements were performed under uniaxial compression on cylindrical specimens (height: ≈1 cm, diameter: ≈1 cm) in equilibrium with salt solutions. The shear modulus G was calculated from the nominal stress, σ (force per unit undeformed cross section), using the relation[22]

$$G = \frac{\sigma}{\Lambda - \Lambda^{-2}} \tag{1}$$

where Λ ($= L/L_0$, where L and L_0 is the height of the deformed and undeformed specimen, respectively) is the deformation ratio. Measurements were performed in the range $0.7 < \Lambda < 1$. Volume change and barrel distortion during the mechanical measurements were not observed.

SANS

SANS measurements were made at the National Institute of Standards and Technology (NIST), Gaithersburg, MD, on the NG3 instrument at incident wavelength 8 Å. PAA and DNA gels prepared in D_2O were placed in sample cells with a 2-mm optical path. The measurements were made at three sample-detector distances: 1.3, 4 and 13 m. This configuration spanned the transfer wave vector range $0.002\ \text{Å}^{-1} < q < 0.3\ \text{Å}^{-1}$, where $q = (4\pi/\lambda)\sin(\theta/2)$, and λ and θ are the wavelength of the incident radiation and the scattering angle, respectively. After azimuthal averaging, corrections for incoherent background, detector response and cell window scattering were applied. The SANS measurements were made below the threshold calcium ion concentration at which phase separation takes place. All measurements were carried out at 25 °C ± 0.1 °C.

ASAXS

ASAXS measurements were made on the BM2 beam line at the European Synchrotron Radiation Facility (ESRF), at five different incident energies 15.800, 16.056, 16.085, 16.097 and 16.102 keV below the absorption edge (16.1046 keV) of Sr. The transfer wave vector range explored was $0.008\ \text{Å}^{-1} \leqslant q \leqslant 1.0\ \text{Å}^{-1}$ and a two-dimensional charge-coupled device (CCD) detector was used. Standard corrections for dark counts, background scattering and camera distortion were made. Intensities were normalized with respect to a standard Lupolen sample of known scattering cross section. Radiation damage was minimized by varying

the sample position at each change of incident energy.[23,24]

In these measurements, two sets of samples were studied: one containing $CaCl_2$ and the other $SrCl_2$. Since Sr is known to mimic the effects of Ca, the ASAXS results from the Sr ions are taken to represent the same distribution as that of Ca ions in these samples. This substitution was adopted because the absorption edge of Ca (4 keV) lies outside the energy range of the BM2 beam line.

the letter Pi is upside down

Results and discussion

Effect of sodium/calcium ion exchange on the macroscopic osmotic and mechanical properties

please place Pi the right way up

To quantify the consequences of monovalent/divalent ion exchange on the macroscopic properties of the gels, we measured the osmotic swelling pressure and the shear modulus of the PAA and DNA gels as a function of the polymer concentration. Osmotic pressure measurements provide insight into the thermodynamic changes that accompany the ion exchange process.

sw

please place Pi the right way up

Figure 1 shows the variation of the swelling degree ($1/\varphi$, where φ is the volume fraction of the polymer) of a PAA gel and a DNA gel in 40 mM NaCl solution as a function of concentration of the two divalent salts ($CaCl_2$ and $SrCl_2$) in the bath with which the gel is in equilibrium.[18,19] Within experimental error, the response to $CaCl_2$ and $SrCl_2$ is identical for each gel. However, although the qualitative behavior of the two gels is similar, their quantitative behavior differs significantly. The PAA gel exhibits a volume transition at approximately 1 mM $CaCl_2$ concentration. In DNA, the volume transition takes place at lower calcium ion content ($\approx$0.25 mM $CaCl_2$) and the volume change is smaller.

please place Pi the right way up

please place Pi the right way up

3

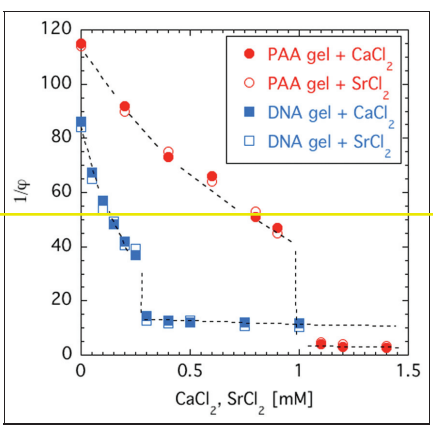

Figure 1. Variation of the swelling degree ($1/\varphi$) of PAA and DNA gels as a function of $CaCl_2$ and $SrCl_2$ concentration in the equilibrium 40 mM NaCl solution.

The essential characteristic of this calcium or strontium ion-induced volume transition is that in both systems, the collapsed gels always completely reswell as the salt concentration is reduced in the equilibrium bath, that is, the transition is *reversible*.

Figure 2 shows the variation of the mixing pressure Π_{mix} of PAA (Figure 2(a)) and DNA gels (Figure 2(b)) as a function of the polymer volume fraction φ in solutions containing 40 mM NaCl and different amounts of $CaCl_2$. Increasing the $CaCl_2$ concentration progressively reduces Π_{mix} in both systems. At a critical threshold concentration, the swelling pressure vanishes and the phase transition commences.

To quantify the effect of calcium ions on the osmotic response, the Π_{mix} curves were analyzed in terms of a modified Flory–Huggins model[25]

$$\Pi_{mix} = \Pi_{\varphi\varphi} + \Pi_{el} = -\left(\frac{RT}{V_1}\right)\left[\ln(1-\varphi) + \varphi + \chi_0\varphi^2 + \chi_1\varphi^3\right] \quad (2)$$

where $\Pi_{\varphi\varphi}$ is the swelling pressure, Π_{el} is the elastic pressure, R is the gas constant, T is the absolute temperature, V_1 is the molar volume of the solvent, and χ_0 and χ_1 are the second- and third-order interaction parameters, respectively. Equation (2) is derived for uncharged gels; in polyelectrolytes, an ion-dependent term must also be included.[26–28] However, previous experimental studies[2–5,29–32] as well as recent molecular dynamics simulations[17] demonstrated that in the presence of added salt, polyelectrolyte solution behavior can still be described by the Flory–Huggins formalism. The simulations show that under equilibrium conditions approximate cancellation arises between the electrostatic contribution and the counterion excluded-volume contribution to the osmotic pressure. Based on these results, it was shown that a modified form of the Flory–Huggins model for nonionic polymer solutions, which accounts for neither electrostatic effects nor counterion excluded-volume effects, fits both experimental and simulated data for polyelectrolyte solutions.[17]

In equation (2), the elastic pressure that counteracts gel swelling can be identified with the shear modulus $\Pi_{el} = -G$ of the gel. The values of G were determined from independent mechanical (uniaxial compression) measurements.

The insets in Figure 2 show the dependence of χ_0 and χ_1 on the calcium chloride concentration. The values of χ_0 and χ_1 were determined from the fits of equation (2) to the osmotic pressure versus polymer volume fraction curves measured at constant $CaCl_2$ concentrations. In both systems, χ_0 is practically unaffected by the calcium ion content. However, χ_1 first exhibits a steep rise, and then, a much weaker increase with increasing $CaCl_2$ concentration, indicating that calcium ions affect primarily the third-order interaction term.

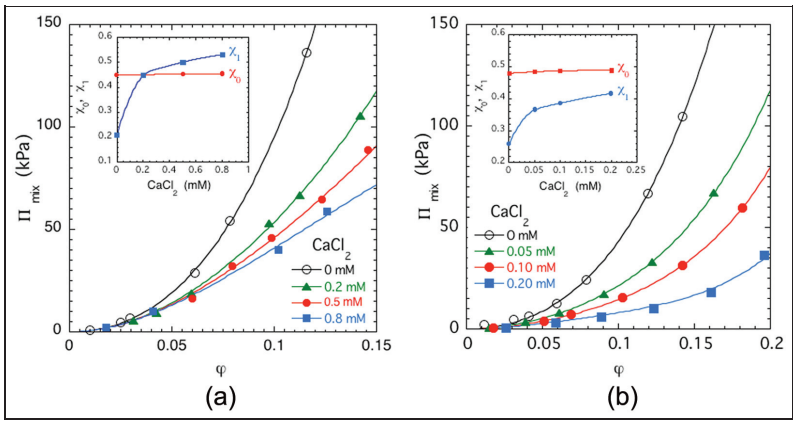

please place Pi the right way up

Figure 2. Dependence of the osmotic mixing pressure Π_{mix} on the polymer concentration in (a) PAA and (b) DNA gels swollen in 40 mM NaCl solution containing different amounts of $CaCl_2$. The continuous curves through the data points are least square fits of equation (2) to the experimental data. Insets: variation of χ_0 and χ_1 with $CaCl_2$ concentration.

Table 1. Elastic moduli of Na-PAA and Na-DNA gels.

Sample	$CaCl_2$ (mM)	φ	*G* (kPa)
PAA	0	0.015	1.6 ± 0.1
PAA	0.8	0.016	1.7 ± 0.1
DNA	0	0.06	0.89 ± 0.05
DNA	0.1	0.07	0.91 ± 0.05

PAA: polyacrylic acid.

The increase in χ_1 with $CaCl_2$ concentration ultimately results in a volume phase transition above a critical threshold value of the divalent salt concentration.

The effect of calcium ions on the elastic response of the gels was determined by measurements of the shear modulus, *G*. This quantity is proportional to the cross-link density. It also varies with the polymer concentration and hence reflects changes in the thermodynamic interaction between the polymer and the solvent. To separate the contribution of the cross-linking density from that of the thermodynamic interactions, mechanical measurements must be made on gel samples that have the same polymer concentration. To satisfy this requirement is not easy because changes in the polymer–solvent interaction affect the swelling equilibrium concentration. In this study, the polymer volume fraction in the gels was adjusted by the osmotic stress technique, which allows us to finely tune the polymer concentration and make modulus measurements on gels at approximately identical polymer volume fractions.

Table 1 lists the values of *G* for PAA and DNA gels measured at comparable concentrations, with and without calcium chloride. While it is known that certain complex-forming ions, such as copper or cobalt, modify the elastic properties of polyelectrolyte gels,[2,4] the results displayed in Table 1 show that calcium ions do not produce additional "cross-links." The observed small increase in *G* is the consequence of the decrease in the swelling degree with increasing $CaCl_2$ concentration. (Note, however, that the present static measurements do not exclude the possibility of temporary bridges of lifetime shorter than the duration of the experiment, since this technique cannot detect them.)

Effect of calcium ions on the organization of polymer chains measured by SANS

To obtain information about calcium ion–induced changes in the organization of polyelectrolyte chains, we made SANS measurements on gels at equilibrium with salt solutions of different concentrations and compositions. Figure 3 shows the SANS signal of PAA and DNA gels swollen in 40 mM NaCl and 100 mM NaCl solutions. Apart from the difference in the scattering intensity due to the different neutron contrast factors of these polymers, the SANS responses are similar. In both systems, a strong increase in $I(q)$ is observed at low values of q. This upturn is a typical feature of polyelectrolyte solutions and gels and is attributed to scattering from clusters of macroions in solution and various types of inhomogeneities. In the low q region, the scattering intensity $I(q)$ can be described by a power law dependence of the form $I(q) \propto q^{-m}$, where $3.2 < m < 3.6$. This response is characteristic of scattering from very rough surfaces: the outer surface of the inhomogeneities is not smooth. In the high q region, a downward curvature of the intensity is visible due to the finite cross-sectional radius of the polymers. In the case of the DNA double helix, its cross-sectional diameter is ≈20 Å, while the cross-sectional diameter of

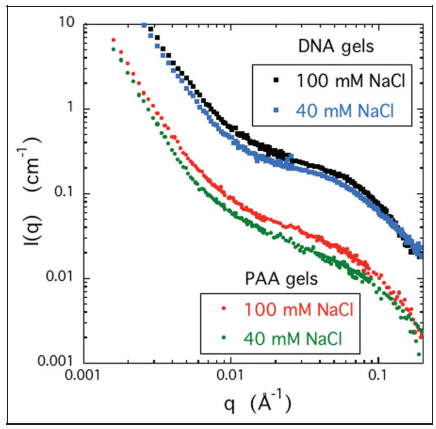

Figure 3. SANS profiles of 3% (w/w) PAA and DNA gels swollen in two different concentrations of NaCl solutions.

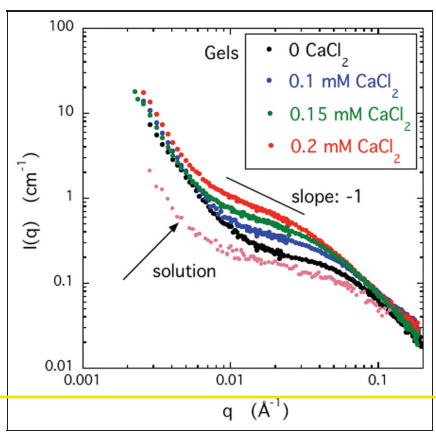

Figure 4. SANS response of 3% (w/w) DNA solution and gels in 40 mM NaCl solution containing different amounts of $CaCl_2$.

PAA is smaller (≈5 Å). The similarity between the shapes of the scattering curves implies that, in spite of differences in chemical composition and flexibility of these molecules, the physical forces that govern the hierarchical organization are the same. It can also be seen that increasing the NaCl concentration from 40 to 100 mM does not change significantly the organization of the polymer chains in these gels.

To distinguish between the structural effects specific to bridging by calcium ions and those that accompany covalent cross-links, Figure 4 shows the influence of calcium ions on the SANS profile of a DNA gel. We see that the addition of calcium chloride does not modify the high q end of the spectrum, that is, the local structure of the molecule is hardly affected. At intermediate length scales, however, the scattering intensity is substantially enhanced. Since this intensity has an osmotic origin, the enhancement extends to the thermodynamic limit $q \rightarrow 0$, where $I(q)$ is defined by

$$I(q)|_{q\rightarrow 0} = \frac{AkT\varphi}{(\partial\Pi/\partial\varphi)} \tag{3}$$

$I(q = 0)$ is, of course, not measured directly, since the direct beam is at $q = 0$: $I(q)|_{q\rightarrow 0}$ is found only by extrapolation. In equation (3), A is a contrast factor, k is the Boltzmann constant and $\partial\Pi/\partial\varphi$ is the osmotic compressibility. The increase in intensity reflects the decrease in $\partial\Pi/\partial\varphi$ with calcium ion concentration as phase separation is approached. In the intermediate q range, the slope of the $I(q)$ versus q curves gradually increases with increasing $CaCl_2$ concentration and approaches -1, which is a characteristic of rod-like scatterers. This slope is consistent with results obtained for other polyelectrolyte systems.[33,34] At low q ($q < 0.05$ Å^{-1}), the invariance of the intensity implies that calcium ions *do not* significantly affect the large-scale structure.

The lowest curve in Figure 4 is that of a DNA solution in 40 mM NaCl, without $CaCl_2$. The scattering intensity is weaker in the solution than in the corresponding gel. The cause of the enhanced intensity from the gel is that cross-links create polymer-rich regions, which generate intense scattering at low q. Between these regions, the polymer concentration is depleted and the osmotic modulus is accordingly reduced. Clearly, this feature distinguishes covalent cross-links from calcium ion–induced changes in the organization of the polymer chains.

At large values of q (small spatial scales), the solution and gel curves tend to coincide, indicating that at high resolution the chain geometry is influenced neither by the chemical cross-links nor by the calcium ions.

increasing calcium ion concentration

In summary, the SANS results show that both ~~"calcium bridging"~~ and covalent cross-linking increase the concentration fluctuations. Calcium ions, however, do not significantly affect the larger scale structures, while chemical cross-linking produces static frozen-in inhomogeneities that strongly increase the scattering intensity in the low q region.

Effect of monovalent/divalent ion exchange on the counterion atmosphere

Osmotic measurements indicate that calcium ions interact with the anionic polymer chains and facilitate attractive forces between them. SANS reveals that divalent counterions strongly modify both the thermodynamic interactions and the supramolecular organization of the chains in polyelectrolyte gels. Although osmotic pressure measurements and SANS provide a means of quantifying important consequences of the monovalent/divalent ion exchange process, they

provide no information about the distribution of divalent ions in the system.

It is known that X-rays interact with the electrons and that the X-ray cross section of atoms increases monotonically with the atomic number. (This behavior is fundamentally different from neutrons, where the interaction with the nucleus of the atoms exhibits no clear trend with atomic number.) Previously, it has been demonstrated that ASAXS can be used to determine how the counterions are distributed in the ionic atmosphere.[23,24,35,36] ASAXS selectively probes the scattering from the counterions. In this experiment, tuning the energy of the incident radiation close to atomic absorption edge modifies the scattering contrast between the counterions and the solvent. Far below the resonant energy (absorption edge), the signal is proportional to the atomic number, while just below the edge, the scattering intensity decreases. Close to the edge, the scattering response contains both resonant (energy dependent) and non-resonant (energy independent) terms. Subtraction of one scattering profile from another removes the energy-independent terms. From the difference signal, after appropriate normalization, the spatial distribution of the counterions (resonant atoms) in the ionic atmosphere around the charged polyelectrolyte chains can be determined. We measured the ASAXS difference profiles of Sr^{2+} in DNA solutions in 100 mM NaCl at six energies (15.800, 15.984, 16.056, 16.085, 16.097 and 16.102 keV) below the strontium absorption edge (16.1046 keV). These data were corrected for the q-independent incoherent scattering associated with the fluorescence near the transition. The $SrCl_2$ concentration varied in the range from 0.011 to 0.111 M (in 0.1 M NaCl).

Figure 5 shows typical small-angle X-ray scattering (SAXS) profiles of DNA containing Sr^{2+} ions (80 mM $SrCl_2$ in 100 mM NaCl) at energies close to the absorption edge of the Sr (16.102 keV, red symbol) and far below the edge (15.800 keV, blue symbol). As the absorption edge of the resonant atom is approached, the scattering intensity decreases. The inset in the figure illustrates the anomalous signal $\Delta I(q)$ obtained by subtracting the response at 16.102 keV, just below that absorption threshold of strontium (16.1046 keV), from that at 15.8 keV, far below it.

Figure 6(a) shows $\Delta I(q)$ for three different $SrCl_2$ concentrations at constant energy of 16.102 keV. The data illustrate that in the low q region, both the intensity of the anomalous scattering signal and the slope of the ΔI versus q plots gradually increase as Sr^{2+} ions replace Na^+ ions in the ion cloud. This trend mimics the variation of the total scattering intensity $I(q)$ with increasing calcium ion concentration as measured by SANS (see Figure 4). The observed behavior is expected through the progressive replacement of Na^+ ions by Sr^{2+} ions. It is noticeable that the position of the steep intensity decrease in the high q region is practically unaffected by the divalent ion concentration. In other words, these

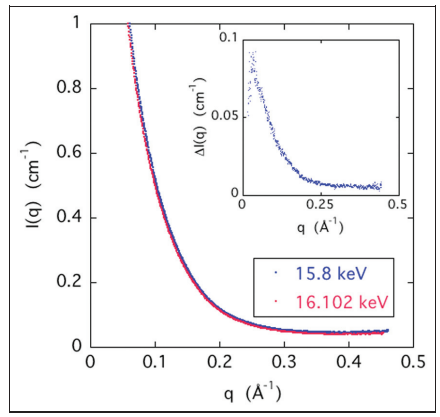

Figure 5. SAXS profiles of 3% (w/w) DNA solution in 80 mM $SrCl_2$ solution close to the absorption edge of Sr^{2+} (16.102 keV) and far below the edge (15.8 keV). The scattering curves are almost indistinguishable in the figure. The inset shows the difference between the two SAXS profiles.

data show no evidence of ion-induced structural changes, such as bridging or intermolecular coupling.

In Figure 6(b), the anomalous scattering response of the DNA sample with 80 mM $SrCl_2$ is displayed in the Kratky representation ($q^2\Delta I$ vs q). Kratky plots highlight the higher angle scattering features and yield structural information on shorter length scales. Two fitting curves are shown. The "solid cylinder" model (blue dashed curve) yields an estimate of the radius of a cylinder that includes both the DNA double helix and its dressing of Sr^{2+} ions in its immediate vicinity $r_1 = 15 \pm 1$ Å. An arguably more physically plausible model consists of a "double cylinder," in which the DNA backbone forms an inner cylindrical core of radius r_2, surrounded by a cylindrical sheath of ions with external radius r_1 (see sketch in Figure 6(b) and Appendix 1). With the values $r_1 = 14 \pm 1$ Å and $r_2 = 9 \pm 1$ Å, this model gives a fit to the experimental data (red continuous curve) of comparable quality to that of the solid cylinder. Larger values of r_2, however, give appreciably poorer fits. Although these simple models, which assume smooth geometrical surfaces, must be viewed with caution, the values found imply that the thickness of the Sr^{2+} ion cloud surrounding the DNA, approximately 5 ± 1 Å, is close to the nominal Debye screening length ($\approx$5 Å). Such a radial constraint does not localize the divalent ions as it permits ion mobility along the polymer chain axis.

The maximum intensity at the peak of the $q^2\Delta I$ versus q representation may be calibrated with respect to the concentration of Sr ions in the ion cloud. This was done by comparing the total SAXS scattering intensity of DNA solutions containing 0.1 M NaCl and $SrCl_2$ with that of equivalent DNA solutions containing 0.1 M NaCl and $CaCl_2$ at the same concentration.

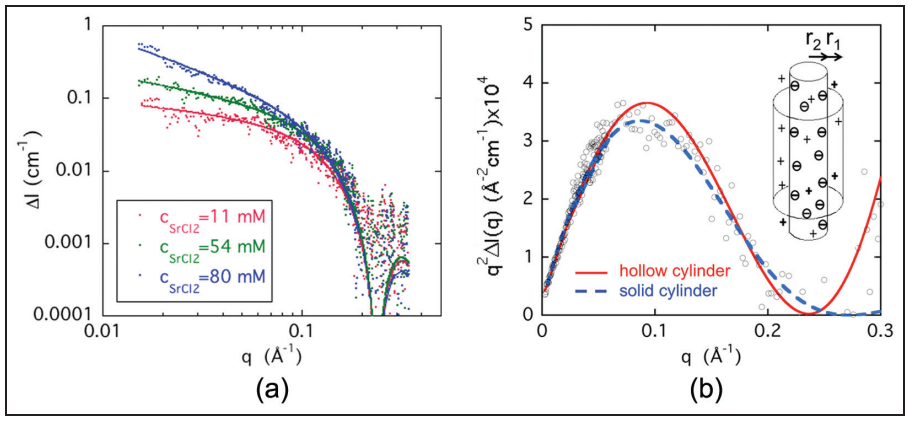

Figure 6. (a) ASAXS profiles of the strontium response from 3% (w/w) DNA solutions containing different amounts of $SrCl_2$ in 100 mM NaCl. (b) Kratky plot ($q^2\Delta I$ vs q) of SAXS measurements in DNA solutions containing 80 mM $SrCl_2$. Lines show the fits to a solid cylinder (dashed curve) and a double cylinder (continuous curve). The schematic diagram shows the cylindrical sheath of ions around the DNA double helix. The negative charges (Θ) are fixed to the perimeter of the inner cylinder of radius r_2, while the positive ions are free to move axially in the space between r_1 and r_2.

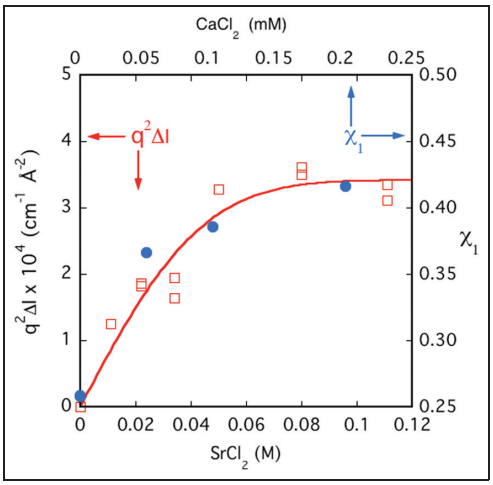

Figure 7. Dependence of the strontium ion concentration in the ion cloud on $SrCl_2$ concentration in the DNA solution (left axis). Variation of the third-order Flory–Huggins interaction term determined from osmotic swelling pressure measurements for DNA gels as a function of the $CaCl_2$ concentration in 100 mM NaCl solution (right axis).

Figure 7 shows that the Sr^{2+} concentration in the ion cloud gradually increases with the $SrCl_2$ content of the system and then levels out above 0.06 M $SrCl_2$ (left axis). Below the condition of saturation, when the DNA is only partially "coated" by divalent ions, it behaves as an ion exchanger.

At the molecular level, ASAXS thus indicates that increasing divalent ion concentration results in their accumulation in the proximity of the charged polyelectrolyte, and that they approach the stoichiometric limit. At the macroscopic level in DNA gels, it was found that the main effect of the calcium ions is to reduce the osmotic pressure by modifying the thermodynamic interaction between the polymer and the solvent through an increase in χ_1 in equation (2) (see Figure 2). To relate these microscopic and macroscopic observations, Figure 7 also displays the variation of χ_1 with $CaCl_2$ concentration for the DNA gels (right axis). The similarity between the two dependences is remarkable. The increase in χ_1 closely follows that of the divalent ion concentration in the counterion cloud, implying that the thermodynamics of this system is governed by the composition of the ion cloud accumulated around the DNA strands. (The concentration of divalent ions in a polyelectrolyte gel is much higher than that in the surrounding bath with which it is in equilibrium, due to the electrostatic attraction between the negatively charged backbone and the positively charged counterions. In the polyelectrolyte solution, however, both the polymer and the ions are distributed throughout the whole volume. This accounts for the difference in the concentration scale for the gels and the solutions in Figure 7.)

In these complex systems, it is known that the counterions screen the repulsive electrostatic interaction, and that the Coulomb attraction between the divalent ions and the negative charges on the polymer backbone may favor pairing between polymer segments belonging to neighboring chains. However, the scattering response in the high q region of the ASAXS measurements reveals no sign of local pairing. Indeed, such local pairing would be unfavorable, since it would reduce the entropy of the divalent ions. Moreover, the absence of measurable increase in the shear modulus indicates that Ca^{2+} ions do not affect the static elastic properties of the present gels (Table 1). The present results, therefore, bring evidence that the polymer chains are decorated

with divalent ions and that the main effect of calcium/strontium ions is to modify the thermodynamics of the system.

Conclusion

An array of experimental techniques probing a wide range of length scales is applied to investigate the effect of divalent/monovalent ion exchange on the structure and thermodynamic properties of a biopolymer and a synthetic polyelectrolyte gel, namely, DNA and PAA. SANS reveals that the calcium ions increase the concentration fluctuations most visibly in the intermediate wave vector range. Comparison between the osmotic pressure of the uncross-linked solution and that of the corresponding gel shows that cross-linking substantially reduces the osmotic pressure. Increasing the calcium chloride concentration has a similar effect on the osmotic pressure. Chemical cross-linking increases the scattering intensity at intermediate length scales and also generates large-scale structural features that, being static, contribute negligibly to the osmotic pressure. The finding that the macroscopic elastic modulus is practically unchanged in the calcium-containing gels demonstrates that calcium ions primarily affect the thermodynamics of the solution rather than network rigidity. It is evident that the main thermodynamic effect is to reduce the repulsion between neighboring polymer chains. ASAXS measurements made on DNA gels indicate that divalent ions are confined inside a cylindrical sheath enveloping the chain.

The results reported here are consistent with a model in which the calcium ions are free to move along the polymer chain, ~~which allows these ions to form temporary bridges~~ between negative charges on adjacent chains. The present observations, however, do not support the hypothesis of "salt bridges."

a situation that can conceivably allow short-lived attractions

Declaration of conflicting interests

The author(s) declared no potential conflicts of interest with respect to the research, authorship and/or publication of this article.

Funding

This work was supported by the intramural research program of the NICHD/NIH. This work was also supported by the National Institute of Standards and Technology, US Department of Commerce, by providing the neutron research facilities used in this work. This work utilized facilities supported by the National Science Foundation under Agreement No. DMR-0944772.

References

1. Tanaka T, Fillmore D, Sun ST, et al. Phase transitions in ionic gels. *Phys Rev Lett* 1980; 45: 1636–1640.
2. Ricka J and Tanaka T. Phase transition in ionic gels induced by copper complexation. *Macromolecules* 1985; 18: 83–85.
3. Horkay F, Tasaki I and Basser PJ. Osmotic swelling of polyacrylate hydrogels in physiological salt solutions. *Biomacromolecules* 2000; 1: 84–90.
4. Horkay F, Tasaki I and Basser PJ. Effect of monovalent-divalent cation exchange on the swelling of polyacrylate hydrogels in physiological salt solutions. *Biomacromolecules* 2001; 2: 195–199.
5. Horkay F and Basser PJ. Osmotic observations on chemically cross-linked DNA gels in physiological salt solutions. *Biomacromolecules* 2000; 5: 232–237.
6. Tasaki I. *Physiology and electrochemistry of nerve fibers*. New York: Academic Press, 1982.
7. Tasaki I. Spread of discrete structural changes in synthetic polyanionic gels: a model of propagation of a nerve impulse. *J Theor Biol* 2002; 218: 497–505.
8. Tasaki I and Byrne PM. Discontinuous volume transition in ionic gels and their possible involvement in the nerve excitation process. *Biopolymers* 1992; 32: 1019–1023.
9. Tasaki I and Byrne PM. Discontinuous volume transition induced by calcium-sodium ion exchange in anionic gels and their neurobiological implications. *Biopolymers* 1994; 34: 209–215.
10. Tasaki I. Abrupt structural changes in polyanionic gels evoked by Na-Ca ion exchange: their biological implications. *Macromol Symp* 2005; 227: 97–104.
11. Tasaki I. Repetitive abrupt structural changes in polyanionic gels: a comparison with analogous processes in nerve fibers. *J Theor Biol* 2005; 236: 2–11.
12. Tasaki I. On the reversible abrupt structural changes in nerve fibers underlying their excitation and conduction processes. In: Pollack GH and Chin WC (eds) *Phase transitions in cell biology*. Berlin: Springer Science + Business Media B.V., 2008, pp.1–21.
13. Muthukumar M. Phase diagram of polyelectrolyte solutions: weak polymer effect. *Macromolecules* 35: 9142–9145.
14. Ghosh K, Carri GA and Muthukumar M. Phase transitions in solutions of semiflexible polyelectrolytes. *J Chem Phys* 2002; 116: 5299–5307.
15. Muthukumar M. Theory of counter-ion condensation on flexible polyelectrolytes: adsorption mechanism. *J Chem Phys* 2004; 120: 9343–9350.
16. Liu S, Ghosh K and Muthukumar M. Polyelectrolyte solutions with added salt: a simulation study. *J Chem Phys* 2003; 119: 1813–1823.
17. Yin DW, Horkay F, Douglas JF, et al. Molecular simulation of the swelling of polyelectrolyte gels by monovalent and divalent counterions. *J Chem Phys* 2008; 129: 154902.
18. Horkay F, Hecht AM and Geissler E. Similarities between polyelectrolyte gels and biopolymer solutions. *J Polym Sci Pol Lett* 2006; 44: 3679–3686.
19. Horkay F, Basser PJ, Hecht AM, et al. Comparative study of scattering and osmotic properties of synthetic and biopolymer Gels. *Macromol Symp* 2007; 256: 80–87.
20. Vink H. Precision measurements of osmotic pressure in concentrated polymer solutions. *Eur Polym J* 1971; 7: 1411–1419.
21. Horkay F and Zrínyi M. Studies on the mechanical and swelling behavior of polymer networks based on the scaling concept. *Macromolecules* 1982; 15: 1306–1310.

22. Treloar LRG. *The physics of rubber elasticity*. 3rd ed. Oxford: Clarendon, 1975.
23. Morfin I, Horkay F, Basser PJ, et al. Adsorption of divalent cations on DNA. *Biophysical J* 2004; 87: 2897–2904.
24. Horkay F, Hecht AM, Rochas C, et al. Anomalous small angle x-ray scattering determination of ion distribution around a polyelectrolyte biopolymer in salt solution. *J Chem Phys* 2006; 125: 234904.
25. Flory PJ. *Principles of polymer chemistry*. Ithaca, NY: Cornell University Press, 1953.
26. English AE, Mafe S, Manzanares J, et al. Equilibrium swelling properties of polyampholytic hydrogels. *J Chem Phys* 1996; 104: 8713–8720.
27. Wolgemuth C, Mogilner A and Oster G. The hydration dynamics of polyelectrolyte gels with applications to cell motility and drug delivery. *Eur Biophys J* 2004; 33: 146–158.
28. Sircar S, Keener JP and Fogelson AL. The effect of divalent vs. monovalent ions on the swelling of Mucin-like polyelectrolyte gels: governing equations and equilibrium analysis. *J Chem Phys* 2013; 138: 014901.
29. Brannon-Peppas L and Peppas NA. Equilibrium swelling behavior of pH-sensitive hydrogels. *Chem Eng Sci* 1991; 46: 715–722.
30. Brannon-Peppas L and Peppas NA. Equilibrium swelling behavior of dilute ionic hydrogels in electrolytic solutions. *J Control Release* 1991; 16: 319–330.
31. Kim B and Peppas NA. Analysis of molecular interactions in poly (methacrylic acid-g-ethylene glycol) hydrogels. *Polymer* 2003; 44: 3701–3707.
32. Peppas NA. *Hydrogels in medicine and pharmacy*. Boca Raton, FL: Chemical Rubber Company, 1986.
33. Horkay F, Hecht AM, Grillo I, et al. Experimental evidence for two thermodynamic length scales in neutralized polyacrylate gels. *J Chem Phys* 2002; 117: 9103–9106.
34. Horkay F, Basser PJ, Londono DJ, et al. Ions in hyaluronic acid solutions. *J Chem Phys* 2009; 131: 184902.
35. Sabbagh I, Delsanti M and Lesieur P. Ionic distribution and polymer conformation, near phase separation, in sodium polyacrylate/divalent cations mixtures: small angle x-ray and neutron scattering. *Annu Rev Biophys Biophys Chem* 1990; 19: 301–332.
36. Das R, Mills TT, Kwok LW, et al. Counterion distribution around DNA probed by solution X-ray scattering. *Phys Rev Lett* 2003; 90: 188103.
37. Neugebauer T. Calculation of the light diffusion of filament chain solutions. *Ann Physik: Berlin* 1943; 42: 509–533.
38. Deutch JM. Light scattering from hollow finite cylinders. *Macromolecules* 1981; 14: 1826–1827.

Appendix I

In a polymer solution composed of a solvent (s), ions (x) and the polymer (p), the small-angle X-ray scattering (SAXS) intensity can be written as

AQ3

I(q,E)=r_0^2
Equal sign missing

$$I(q,E)r_0^2\left[\left(\rho_p-\rho_s\right)^2 S_{pp}(q)+2\left(\rho_p-\rho_s\right)\left(\rho_x(E)-\rho_s\right) S_{xp}(q)+\left(\rho_x(E)-\rho_s\right)^2 S_{xx}(q)\right] \quad (4)$$

where r_0 (2.818×10^{-13} cm) is the classical radius of the electron, E is the energy of the incident X-ray beam and the ρ_k are electron densities of the components (k). The $S_{jk}(q)$ are the structure factors of the different components. In the vicinity of the absorption edge, $\rho_x(E)$ is energy dependent. The anomalous small-angle X-ray scattering (ASAXS) measurement is based on the intensity difference

$$\Delta I(q,E_1,E_2)=I(q,E_1)-I(q,E_2)=r_0^2\Big\{2\left(\rho_p-\rho_s\right)[\rho_x(E_1)-\rho_x(E_2)]S_{xp}(q)+[\rho_x(E_1)-\rho_x(E_2)][\rho_x(E_1)+\rho_x(E_2)-2\rho_s]S_{xx}(q)\Big\} \quad (5)$$

To represent the shape of the counterion cloud around the cylindrical DNA molecule, the expression for an infinitely long cylinder of radius r_1 can be used, that is, a simple solid cylinder, with

$$\Delta I(q)\propto\frac{[J_1(qr_1)/q]^2}{q} \quad (6)$$

where $J_1(x)$ is the cylindrical Bessel function of first order.

For a cylinder of finite length L and radius r_1, the approximation adopted is

$$\Delta I(q)=\frac{[J_1(qr_1)/q]^2}{[1+q^2L^2]^{1/2}} \quad (7)$$

in which the denominator is an approximation for the exact Neugebauer expression,[37] and $J_1(x)$ is the cylindrical Bessel function of first order. The parameters obtained from this expression correspond to the *solid cylinder model*.

For the case of a cylindrical shell of ions surrounding the polymer chain (inner radius r_2 and outer radius r_1), the signal consists of two terms: the direct scattering $S_{xx}(q)$ from the shell itself and the interference term $S_{xp}(q)$ between the ions and the inner cylinder, that is, the polymer itself.

These terms are, respectively, for the shell of the long hollow cylinder[38]

$$S_{xx}(q)=\frac{\left[r_1^2J_1(qr_1)-r_2^2J_1(qr_2)\right]^2}{\left[\left(r_1^2-r_2^2\right)^2q^3\right]} \quad (8)$$

When $r_2=0$, this expression tends to equation (6).

The interference term is the product of the *amplitudes* of $S_{xx}(q)$ for the full cylindrical core of the polymer and that of the cylindrical shell of ions

$$S_{xp}(q)\propto\left[r_1^2J_1(qr_1)-r_2^2J_1(qr_2)\right]\times\frac{J_1(qr_2)}{\left[\left(r_2^2-r_2^2\right)r_2q^3\right]} \quad (9)$$

The total intensity is, therefore, the sum of equations (4) and (5), in which the coefficient of term 5 may be either positive or negative since the difference in electron density $[\rho_x(E_1)+\rho_x(E_2)-2\rho_s]$ between the solvent and resonant species in the ion cloud depends both on

the energy E of the incident beam and on the ion concentration in the cloud.

The total fitting function in the double cylinder model is thus

$$\Delta I(q) = \left\{ a\left[r_1^2 J_1(qr_1) - r_2^2 J_1(qr_2)\right]^2 \Big/ \left[\left(r_1^2 - r_2^2\right)^2 q^3\right] + b\left[r_1^2 J_1(qr_1) - r_2^2 J_1(qr_2)\right] \times J_1(qr_2) \Big/ \left[\left(r_1^2 - r_2^2\right) q^3\right] \right\} \Big/ \left[1 + q^2 L^2\right]^{1/2} \quad (10)$$

where a and b are adjustable.